# Determination of the NETD Parameter Value of the Imaging System with a Single MWIR Detector for $CO_2$ Detection

Sebastian Urbaś, Robert Olbrycht, Bogusław Więcek
Lodz University of Technology, Institute of Electronics, Al. Politechniki 6, 90-924 Lodz, Poland

Abstract: This research presents the experimental assessment of the NETD parameter for an infrared system developed for gas detection using the single-pixel imaging technique. Gas imaging systems often uses the narrow-band filtering for contrast enhancement which significantly reduces the incoming radiation energy and deteriorates the signal-to-noise characteristic. The developed system was tested for $CO_2$ detection in MWIR wavelength band. The presented results confirmed experimentally the higher value of the NETD parameter for the system equipped with the interference filter. The NETD parameter was evaluated using a simple testing stand with the black body for selecting the proper background temperature. The obtained results confirm the importance of the background temperature in the detection process, the value of which is important in determining the sensitivity and noise level of the system, the attenuation of the radiation of optical elements and the spectral characteristics of the detected gas.

**Keywords:** single-pixel imaging, gas detection, NETD parameter, MWIR, Spatial Light Modulator

## 1. Introduction

A thermal imaging camera is a device that detects infrared radiation and converts it into a visible image. One of the parameters that significantly affects the quality of thermal image is the NETD (*Noise Equivalent Temperature Difference*) [1]. The NETD parameter indicates the smallest temperature difference the detector can distinguish, typically expressed in mK [2].

Nowadays, the NETD value of a typical the infrared (IR) imaging system is between 30 mK and 100 mK. Generally, thermal cameras with the NETD below 50 mK are used for high-precision detection and measurement. The NETD is crucial parameter in gas detection processes [3]. Too high value of NETD can make gas difficult to distinguish from noise.

A thermal imaging camera doesn't "see" gas directly. It records radiation of the background attenuated by the gas. In order to detect gas with a thermal imaging system, an appropriate narrow-bandpass filter must be used. The $CO_2$ gas has characteristic absorption band in both the Mid-Wave Infrared (MWIR) and the Long-Wave Infrared (LWIR) bands [4]. In practice, the existing IR systems use most often use the wavelength range of approximately 4.2–4.4 µm.

Currently, Optical Gas Imaging (OGI) techniques use thermal imaging cameras with a detector matrix [5]. The novel technique of OGI may use so-called single-pixel imaging (SPI). The SPI systems use only a single-detector [6]. An important element of this solution is the Spatial Light Modulator (SLM) which generates time-varying mask patterns (e.g. with Hadamard or Random templates) [5, 7]. The SLM has a significant impact on the imaging speed, resolution and wavelength. There are several types of SLMs. The *Digital Micromirror Device* (DMD) is the commonly used chip for single-pixel imaging [8]. The DMD consist of thousands of electrically controlled micromirrors that selectively redirect beams of radiation onto a single detector [9, 17]. The advantage of using DMD system is high-speed imaging and the high resolution. Unfortunately, disadvantage of DMD [10] is the limited wavelength range, typically to visible and near-IR bands [11]. Changing the mask patterns over time causes the change in the signal recorded by the single detector, which corresponds to the radiation passing through the SLM modulator [12]. The recorded signal is used to reconstruct an image using appropriate algorithms among others presented in the publication *Review on infrared single-pixel imaging, Opto-Electronics Review* [5]. Recently, *Artificial Intelligence* (AI) algorithms have been used more and more often [13]. The AI algorithms are effective in eliminating noise in images and augmenting their resolution [14].

**Autor korespondujący:**
Sebastian Urbaś, sebastian.urbas@dokt.p.lodz.pl

**Artykuł recenzowany**
nadesłany 07.07.2025 r., przyjęty do druku 11.08.2025 r.

## 2. Measurement method and test rig

Noise Equivalent Temperature Difference (NETD) is the important parameter of an IR systems defining the radiation signal change equal to the noise level defined by the standard deviation. In other words, the NETD refers to the minimum signal that can be detected, i.e. in case of signal-to-noise ratio S/N = 1. According the standard [15], the NETD should be measured at object with uniformly distributed temperature BB (Black Body) equal to 30 °C.

Assuming that the output signal of an IR system is voltage $u$, NETD can be expressed as:

$$NETD = \frac{\sigma}{R_u} = \frac{\sigma}{\frac{du}{dT}}, \quad (1)$$

where: $\sigma$ – standard deviation of the output signal noise (V), $R_u = \frac{du}{dT}$ – system temperature sensitivity of the output voltage expressed in V/K.

The NETD of imaging systems depends on many factors, mainly on the IR detector radiometric characteristics, but also on the parameters of the entire optical path, electronic acquisition system and the black body itself (radiation source). One of the element of the IR system for gas detection in the optical path is a narrow-band filter used for contrast enhancement. It attenuates the incident radiation significantly causing the sensitivity loss. In results, it has an impact on the NETD.

The Single-Pixel Camera (SPC) for gas detection are equipped with a narrow-band filter with transmission characteristic corresponding to the $CO_2$ absorption wavelength band (about 4.26 µm). The transmission bandwidth of the filter that was used in this research is in the range 4191–4341 nm as presented in Fig. 1. The interference filter was made of sapphire, which provides high mechanical and thermal resistance. The filter blocks radiation up to 6 µm, which eliminates a wide range of background energy. The FWHM (*Full Width at Half Maximum*) parameter is 150 nm and CWL (*Central Wavelength*) is 4266 nm [18].

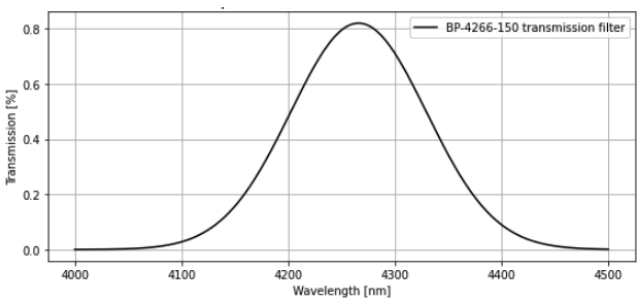


**Fig. 1. Characteristics of narrow-band filter used for $CO_2$ gas detection**
Rys. 1. Charakterystyka filtra wąskopasmowego zastosowanego do detekcji gazu $CO_2$

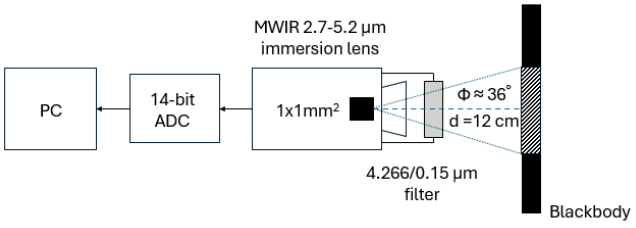


**Fig. 2. Block diagram of test rig used NETD measurement of a single-detector IR system**
Rys. 2. Schemat blokowy stanowiska testowego służącego do pomiaru NETD dla pojedynczego detektora IR

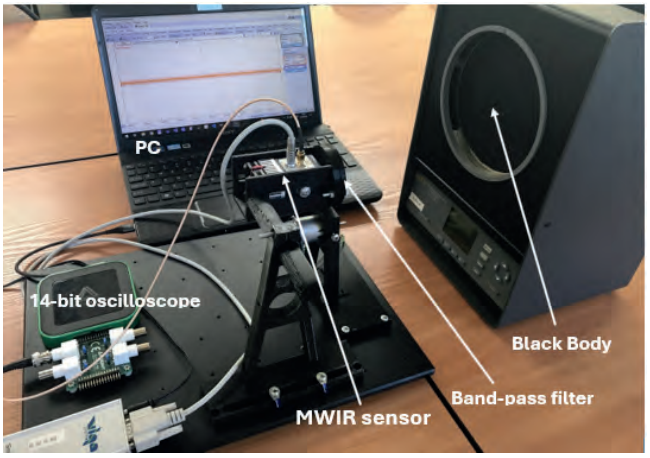


**Fig. 3. Laboratory stand for measuring the NETD parameter of the MWIR sensor**
Rys. 3. Stanowisko laboratoryjne do pomiaru NETD detektora MWIR

The NETD parameter was analyzed by the system with the single MWIR detector shown in Fig. 2. The spectral range of the detector absorption band is from 2.7 µm to 5.2 µm [19]. The optical surface of the photovoltaic detector is 1 × 1 mm², while the field of view (FOV) is 36°. The NETD parameter was tested in two configurations – with and without filter. The BB was placed in front of the detector at a distance of 12 cm, so that the active area of the BB covers the entire detector's FOV. The BB is equipped with a precise temperature control system. The uniformity is ±0,10 °C at 35 °C over the entire surface of the BB aperture. The stability of the BB is ±0,05 °C at 35 °C. The BB stabilization time is 10 minutes [20].

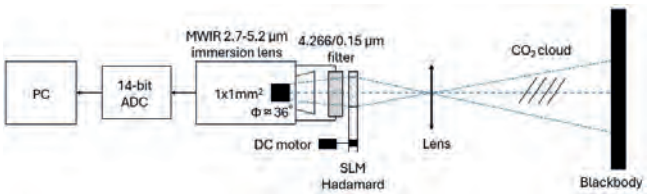


**Fig. 4. Block diagram of the single-pixel IR imaging system for $CO_2$ gas detection**
Rys. 4. Schemat blokowy jednopikselowego systemu obrazowania IR do detekcji gazu $CO_2$

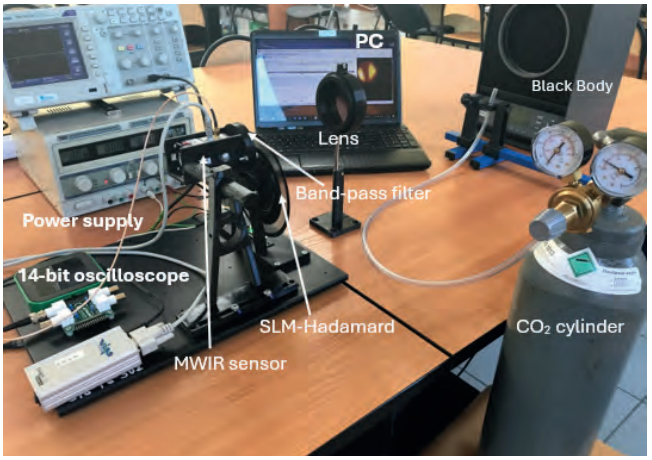


**Fig. 5. Station for detecting CO2 gas leaks using an MWIR sensor**
Rys. 5. Stanowisko do wykrywania wycieku gazu CO2 za pomocą detektora MWIR

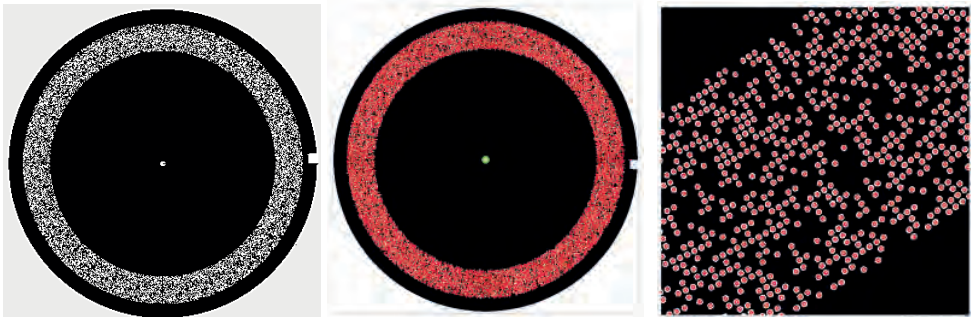

a) b) c)

**Fig. 6. a) Generated SLM modulator with Hadamard mask; b) drill files prepared according to Excellon 2 format and "placed on" the Hadamard mask; c) close-up of the modulator aperture fragment – hole diameter 0.3 mm**

Rys. 6. a) Wykonany modulator SLM z maską Hadamarda; b) pliki wierceń przygotowane w formacie Excellon 2 i „nałożone" na maskę Hadamarda; c) zbliżenie na fragment apertury modulatora – średnica otworu 0,3 mm

For the NETD measurement with the filter, the BB temperature was set between 80 °C and 220 °C. Without the filter, the BB temperature ranged from 30 °C to 150 °C. In both cases the detector signal was recorded every 20 °C.

The block diagram in Fig. 4 shows the concept of single-pixel imaging for $CO_2$ gas detection. A narrow band-filter was mounted just in front of the single-detector.

The SLM modulator with Hadamard pattern apertures of 31 × 29 resolution was mounted on the DC motor axis. The rotation frequency of the modulator was ~30 rps (rotations per second). A lens was placed in front of the modulator to project IR radiation onto the modulator's aperture. Between the BB and the lens there was a tube connected to the $CO_2$ cylinder filled with the compressed gas. The $CO_2$ gas was observed based on the thermal contrast caused by the strong attenuation of radiation in MWIR range.

The SLM modulator was manufactured with a previously prepared script written in MATLAB software. The result of the developed program was SLM file saved as an image in the *slm.png* format. Next, the target dimension of the SLM (16 cm radius) were set in the GIMP software [21]. The *slm.png* was imported into the online converter files – *reaconverter*, whose purpose was to convert the *slm.png* file into a file in the *gerber* format widely used in PCB production [22]. In the next step, the script *drill_generator.m* was used to generate the drilling information for the PCB production. The purpose of the script was to prepare a drilling holes document that complies with the guidelines for the *Excellon 2* format – Fig. 6b [23]. The production of the SLM modulator from aluminum was outsourced to an external company. The drilled holes diameter was set at 0.3 mm – Fig. 6c.

SLM modulators were made of photographic film and aluminum thin plate as presented in Fig. 7. The dimensions of these 2 SLMs are identical and both were used in the experiments. The diameter in both cases was Ø = 16 cm. The aluminum modulator has a low emissivity value and introduces signal distortions. For this reason, no tests were carried out with an aluminum modulator. It was presented as an alternative modulator solution for future research. In both produced SLMs, the Hadamard pattern matrix was used to modulate spatially the radiation coming from an object. An important feature of the Hadamard matrix is its cyclicity. In result, shifting the SLM matrix by one pixel preserves the Hadamard template. The size of a single aperture on the SLM disk was 31 × 29. The size of the entire Hadamard matrix was 899 × 899 with rows defining each aperture of the SLM. The Hadamard matrix was generated using the twin-prime numbers algorithm [17].

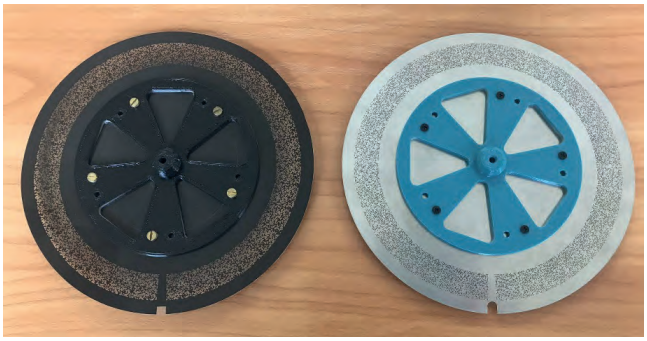

**Fig. 7. Two types of SLMs – from the left made of photographic film and on the right made of aluminum**

Rys. 7. Dwa rodzaje modulatorów SLM – po lewej wykonany z kliszy fotograficznej, po prawej z aluminium

## 3. Results

In order to evaluate the NETD parameter, the histograms were calculated for long sequences of output samples. Recording these sequences were made using the system shown in Fig. 3. Examples of the histograms with and without filter are presented in Fig. 8. They show measured voltage distribution of the recorded sequence of 32,768 samples of the output signal.

Quantitative results presenting the statistical parameters of the recorded data and estimated NETD values for experimental data with and without a filter mounted next to the detector are summarized in the tables 1 and 2. As expected, the average output signal grows with the BB temperature while its standard deviation for the detector with the narrow band filter remains almost the same. It denotes that the noise level does not affect the NETD of the IR system with filter significantly. Removing the filter placed in front of the detector increases noise in the high BB temperature range. This effect can be explained by strong radiation attenuation of the filter almost in the entire wavelength bandwidth of the detector absorption characteristic. Increasing the BB temperature causes the strong air movement due to the natural convection near the radiation surface and in consequence it increases the noise of the incoming signal.

On the other hand, the value of NETD is much lower for the system without filter. This an obvious conclusion as the signal and its derivative is much higher. The derivative which is in the denominator in the equation (1) can be roughly estimated in Fig. 9 presenting the dependence of the output voltage signal of the detector vs. temperature of the BB. In addition, Fig. 9 shows

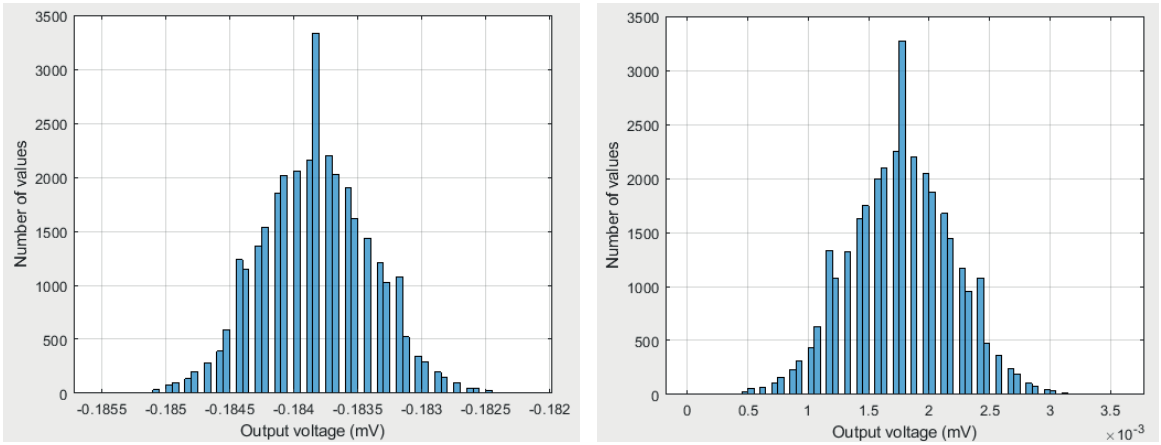


a) b)

**Fig. 8. Measured output voltage histograms for the single-detector: a) with IR filter and BB temperature of 100 °C; b) and without IR filter and BB temperature of 50 °C**

Rys. 8. Histogramy zmierzonego napięcia wyjściowego na pojedynczym detektorze: a) z filtrem IR i temperaturą BB 100 °C; b) oraz bez filtra IR i temperatury BB 50 °C

**Table 1. Output Voltage, standard deviations, and NETD parameters for a system with single detector and IR Filter**

Tabela 1. Wartości średnie napięcia wyjściowego, odchylenia standardowe i parametry NETD dla systemu z pojedynczym detektorem i filtrem IR

| Temp. BB (°C) | Average voltage (V) | Standard deviation (V) | NETD (K) |
|---|---|---|---|
| 80 | –0.200 | 0.000411 | 1.190 |
| 100 | –0.183 | 0.000426 | 0.509 |
| 120 | –0.162 | 0.000425 | 0.320 |
| 130 | –0.147 | 0.000444 | 0.282 |
| 150 | –0.115 | 0.000432 | 0.209 |
| 170 | –0.0703 | 0.000435 | 0.170 |
| 180 | -0.0418 | 0.000439 | 0.157 |
| 200 | 0.0172 | 0.000431 | 0.131 |
| 220 | 0.0927 | 0.000445 | 0.117 |

both the curves of the output signal vs. temperature of the BB for the experiments with and without filter. In result, it allows to compare the both levels of the output voltage and estimate the average system sensitivities in both cases. It can be noticed that the sensitivity changes nonlinearly and is higher for higher BB temperature. This is the reason why the NETD becomes lower for higher temperature of the observed scene. The single-pixel system with an MWIR detector with transimpedance amplifier generates negative and positive voltages.

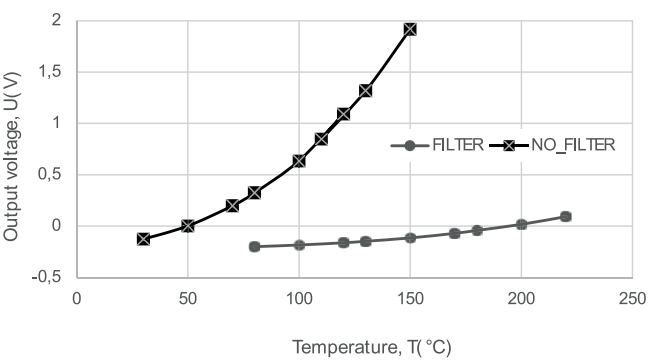


**Fig. 9. Output voltage measured on a single-detector with and without IR filter for different BB temperature**

Rys. 9. Napięcie wyjściowe mierzone na pojedynczym detektorze z filtrem IR oraz bez filtra IR dla różnych temperatur BB

Figure 9 shows the dependence of the detector output voltage vs. of BB temperature. Each point is the average value of the detector output voltage measured over time.

The approximation function for the output voltage detector without a filter takes the form:

$$u(T) = 0.1175\,T^2 - 4.3287\,T - 88.845 \tag{2}$$

and its derivative is expressed as:

$$\frac{du}{dT} = R_u(T) = 2 \cdot 0.1175\ T - 4.3287. \tag{3}$$

In contrast, the approximation function for the output voltage detector with the filter:

$$u(T) = 0.0123\,T^2 - 1.6227\,T - 146.06 \tag{4}$$

**Table 2. Output Voltage, standard deviations, and NETD parameters for a system with single detector without IR Filter**
Tabela 2. Wartości średnie napięcia wyjściowego, odchylenia standardowe i parametry NETD dla systemu z pojedynczym detektorem bez filtra IR

| Temp. BB (°C) | Average voltage (V) | Standard deviation (V) | NETD (K) |
|---|---|---|---|
| 30 | –0.127 | 0.000424 | 0.156 |
| 50 | 0.0018 | 0.000426 | 0.0574 |
| 70 | 0.197 | 0.000433 | 0.036 |
| 80 | 0.324 | 0.000447 | 0.031 |
| 100 | 0.636 | 0.000493 | 0.026 |
| 120 | 1.093 | 0.000604 | 0.025 |
| 110 | 0.848 | 0.000502 | 0.023 |
| 130 | 1.318 | 0.000522 | 0.020 |
| 150 | 1.917 | 0.000754 | 0.024 |

and the derivative of the function:

$$\frac{du}{dT} = R_u(T) = 2 \cdot 0.0123\ T - 1.6227. \tag{5}$$

In both cases the coefficient of determination ($R^2$) of the approximating functions is $R^2 > 0.999$.

In Figure 10 shows the quantitative results of the NETD parameter for the system with a single MWIR. The NETD analysis was performed for the measurement system with and without the IR filter. It can be seen that the use of the filter significantly worsens the NETD (Table 1, 2 and Fig. 10). It turns out that the filter significantly attenuates the signal. For the system with a filter, the NETD level becomes acceptable above the BB temperature of 220 °C and is 117.43 mK. For a system without filter, as the background temperature increases, the NETD improves. At a temperature of 30 °C the NETD is 155.80 mK and for the maximum tested BB temperature of 150 °C the NETD is 24.38 mK.

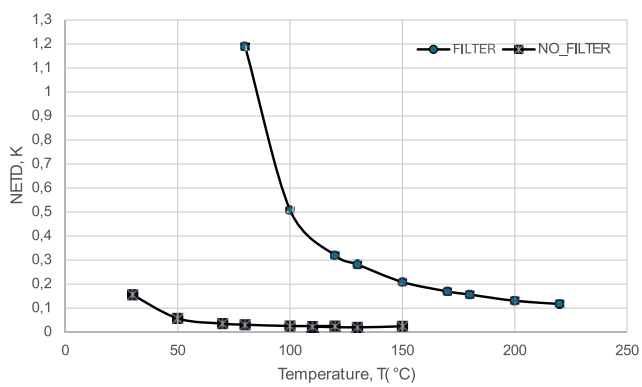


**Fig. 10. NETD parameter for the single MWIR detector with and without filter**
Rys. 10. Parametr NETD dla pojedynczego detektora MWIR z filtrem i bez filtra

Finally, the sample IR images taken with the single detector system for different BB temperature are presented in Fig. 11. Detection of $CO_2$ gas below a background temperature of 200 °C becomes almost impossible. There is too much noise in the image, preventing proper gas identification as it is visible in Fig. 11c.

It has to be noticed that the low-cost SLM modulator made of photographic film is a weakest element of the SPC system for gas detection. It is not perfectly flat and it can bend during rotation. Moreover, the system requires the very precise control and stabilization of the rotation speed of the SLM and the precise synchronization of the SLM rotation with the signal acquisition. The narrow band IR filter attenuates the incoming radiation and in result it deteriorates the sensitivity of the system with decrease of NETD simultaneously.

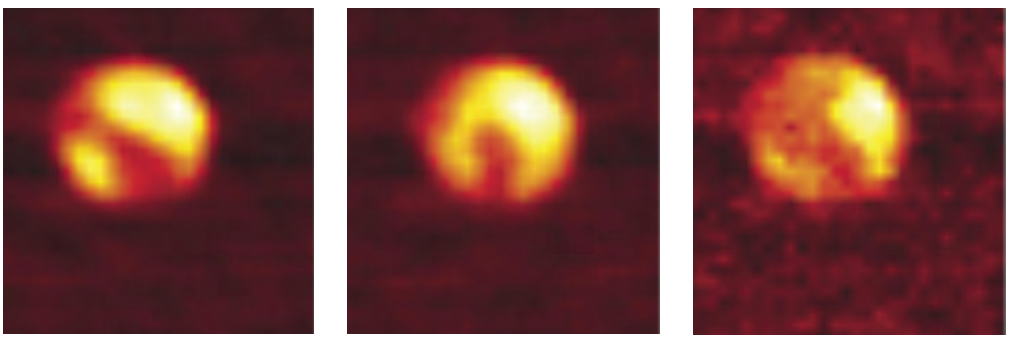

a) b) c)

**Fig 11. Example of IR image with a $CO_2$ gas leak for different temperature of BB: a) 400 °C, b) 300 °C, c) 200 °C**
Rys. 11. Przykładowe obrazy IR z wyciekiem gazu $CO_2$ dla różnej temperatury tła (BB): a) 400 °C, b) 300 °C, c) 200 °C

## 4. Conclusion

Gas detection and measurement of the concentration can be implemented using IR system equipped with the narrow-band interference filter with the spectral characteristic correlating to the gas absorption. Single-pixel imaging technique is a cost-effective solution allowing to exchange the filter to detect different gas atmospheres. The main problem of such a technique is the background temperature that sometimes must be high. In practice it limits the field of applications, especially while using it in the explosive environment. The right solution is to select the highly sensitive IR system with low value of the NETD parameter. In this research we presented a simple method of NETD assessment that can be implemented in-house by the user of an infrared system. It only requires a heat source (e.g. the black body) with adjustable temperature. The presented results confirmed importance of the noise and the sensitivity characteristics of the IR system used for gas detection. These parameters has an impact on the background temperature during the gas detection that can often be above 100 °C. The narrow-band filter that is an important part of the system that reduces the NETD parameter significantly. In the presented research the IR system without any filter had NETD = 157 mK@30 °C and NETD = 1190 mK@80 °C while narrow-band was used. When background temperature was increased, the NETD figures become much better achieving NETD = 117 mK@220 °C and NETD = 24 mK@150 °C for the system with and without radiation filtering. It has to be underlined that these results were obtained for the cooled $1 \times 1$ mm$^2$ MWIR sensor equipped with the immersive integrated lens and 4-stage thermoelectric cooler allowing to diminish the detector temperature to about –40 °C. Such a detector can be successfully used for $CO_2$ detection and the concentration measurement using single-pixel imaging when the background temperature is above 200 °C. Single detector systems are used among others in medical imaging, petrochemistry and gas leak detection.

## References


1. Więcek B., De Mey G., *Termowizja w podczerwieni podstawy i zastosowania*, Wydawnictwo PAK, Warszawa 2011, 103–130, ISBN 978-83-926319-7-2, 29–32.
2. Gogler S., Sawicki K., Ligienza A., Mścichowski M., *Metoda pomiaru minimalnej rozróżnialnej różnicy temperatury w funkcji powiększenia i rozogniskowania kamery termowizyjnej*, „Pomiary Automatyka Robotyka", R. 28, Nr 2, 2024, 99–106, DOI: 10.14313/PAR_252/99.
3. Mścichowski M., Sawicki K., Sosnowski T., Firmanty K., Kastek M., Bareła J., *Metoda pomiaru parametrów kamer termowizyjnych za pomocą zautomatyzowanego stanowiska pomiarowego*, „Pomiary Automatyka Robotyka", R. 28, Nr 3, 2024, 131–138, DOI: 10.14313/PAR_253/131.
4. Olbrycht R., *A novel method for sensitivity modelling of optical gas imaging thermal cameras with warm filters*, "Quantitative InfraRed Thermography Journal", Vol. 19, No. 5, 2022, 331–346, DOI: 10.1080/17686733.2021.1962096.
5. Szajewski K., Szajewska A., Urbaś S., Więcek B., *Review on infrared single-pixel imaging*, "Opto-Electronics Review", Vol. 33, No. 2, 2025, DOI: 10.24425/opelre.2025.154306.
6. Gibson G.M., Johnson S.D., Padgett M.J., *Single-pixel imaging 12 years on: a review*, "Optics Express", Vol. 28, No. 19, 2020, 28190–28208, DOI: 10.1364/OE.403195.
7. Wang Y., Huang K., Fang J., Yan M., Wu E., Zeng H., *Mid-infrared single-pixel imaging at the single-photon level*, "Nature Communications", Vol. 14, 2023, DOI: 10.1038/s41467-023-36815-3.
8. Duarte M.F., Davenport M.A., Takhar D., Laska J.N., Sun T., Kelly K.F., *Single-pixel imaging via compressive sampling*, "IEEE Signal Processing Magazine", Vol. 25, No. 2, 2008, 83–91, DOI: 10.1109/MSP.2007.914730.
9. Tissot J.L., *Uncooled infrared detectors: state of the art*, VII Krajowa Konferencja Termografia i Termometria w Podczerwieni TTP 2006, Ustroń-Jaszowiec, 16–18 listopada, 2006, 9–23.
10. Yoon T., Kim C.-S., Kim K., Choi J., *Emerging applications of digital micromirror devices in biophotonic fields*, "Optics & Laser Technology", Vol. 104, 2018, 17–25, DOI: 10.1016/j.optlastec.2018.02.005.
11. Carlos Osorio Quero, Daniel Durini, Jose Rangel-Magdaleno, Jose Martinez-Carranza, and Ruben Ramos-Garcia, *Deep-learning blurring correction of images obtained from NIR single-pixel imaging*, "Journal of Optical Society of America A", Vol. 40, No. 8, 2023, 1491–1499, DOI: 10.1364/JOSAA.488549.
12. Nobunaga T., Tanaka H., Tadokoro Y., *Reconstruction for Spatially Distributed Single-Pixel Imaging Based on Pattern Filtering*, "IEEE Signal Processing Letters", Vol. 25, No. 5, 2018, 705–709, DOI: 10.1109/LSP.2018.2816579.
13. Urbaś S., Więcek B., *Application of a deep-learning neural network for image reconstruction from a single-pixel infrared camera*, "Opto-Electronics Review", Vol. 32, No. 1, 2024, DOI: 10.24425/opelre.2024.148877.
14. Song K., Bian Y., Wang D., Li R., Wu K., Liu H., Qin C., Hu J., Xiao L., *Advances and Challenges of Single-Pixel Imaging Based on Deep Learning*, "Laser & Photonics Reviews", Vol. 19, No. 7, 2025, DOI: 10.1002/lpor.202401397.
15. Minkina W., Dudzik S., *Infrared Thermography, Errors and Uncertainties*, Częstochowa University of Technology, 2009.
16. Harwit M., Sloane N.J.A., *Hadamard Transform Optics*, 1979, DOI: 10.1016/B978-0-12-330050-8.X5001-X.


## Other sources


17. [www.ti.com/lit/an/dlpa008b/dlpa008b.pdf].
18. [www.spectrogon.com/products/ir-filters-for-gas-analysis-2].
19. [https://vigophotonics.com/].
20. [www.fluke.com/pl-pl/produkt/przyrzady-do-kalibracji/kalibratory-temperatury/fluke-calibration-4180-4181].
21. [www.gimp.org].
22. [www.pcbcart.com/article/content/PCB-manufacturing-process.html].
23. [https://jlcpcb.com/help/article/Manually-Adding-Tool-List-for-a-Drill-File].

# Wyznaczanie wartości parametru NETD systemu obrazowania z pojedynczym detektorem MWIR do detekcji $CO_2$

Streszczenie: W pracy przedstawiono eksperymentalną ocenę parametru NETD dla systemu podczerwieni MWIR opracowanego do wykrywania gazów przy użyciu techniki obrazowania jednopikselowego. W systemach obrazowania gazów często stosowane jest filtrowanie wąskopasmowe w celu zwiększenia kontrastu, co znacznie zmniejsza energię promieniowania i pogarsza charakterystykę sygnału względem szumu. Opracowany system przetestowano pod kątem wykrywania CO2 w paśmie fal średniej podczerwieni (MWIR). Przedstawione wyniki potwierdziły eksperymentalnie wyższą wartość parametru NETD dla układu wyposażonego w filtr interferencyjny. Parametr NETD oceniano przy użyciu prostego stanowiska pomiarowego z ciałem czarnym, co pozwalało na wybór właściwej temperatury tła. Uzyskane wyniki potwierdzają znaczenie temperatury tła w procesie detekcji, której wartość jest istotna przy wyznaczaniu czułości i poziomu szumów systemu, tłumienia promieniowania elementów optycznych i charakterystyki widmowej wykrywanego gazu.

**Słowa kluczowe:** obrazowanie jednopikselowe, detekcja gazu, parametr NETD, MWIR, modulator SLM

## Sebastian Urbaś, MSc Eng.
sebastian.urbas@dokt.p.lodz.pl
**ORCID: 0000-0002-7699-5425**

He graduated with an engineering degree in computer science in 2019 from the University of Academy of Social and Media Culture in Toruń. In 2021 he received a master's degree in electronics from the Lodz University of Technology. Currently, he is a PhD student at the Lodz University of Technology. The main areas of interest are embedded electronics, computer thermography, signal and image processing and development of IR systems., PLC and SCADA systems.

## Robert Olbrycht, PhD Eng.
robert.olbrycht@p.lodz.pl
**ORCID: 0000-0001-9842-2815**

He received the PhD degree in electronic engineering from the Lodz University of Technology, Lodz, Poland, in 2012. He is currently an Assistant Professor of Electronics with the Institute of Electronics, Lodz University of Technology. He has published papers on optical gas imaging with thermal imaging cameras and applications of thermography for industrial purposes.

## Prof. Bogusław Więcek, DSc PhD Eng.
boguslaw.wiecek@p.lodz.pl
**ORCID: 0000-0002-5003-1687**

Prof. Bogusław Więcek is the head of the Department of Electronic Circuits and Thermography at the Institute of Electronics of the Lodz University of Technology. He specializes in computer thermography and modeling of thermal problems in electronic systems. He is a member of the scientific committee of the international Conference on Quantitative Infrared Thermography (QIRT) and chairman of the Conference on Infrared Thermography and Thermometry organized periodically in Poland.